Biosensors and Bioelectronics 80 (2016) 294–299

Contents lists available at ScienceDirect

Biosensors and Bioelectronics

journal homepage: www.elsevier.com/locate/bios

# Realization of a label-free electrochemical immunosensor for detection of low density lipoprotein using NiO thin film

Gurpreet Kaur [a], Monika Tomar [b], Vinay Gupta [a,*]

[a] Department of Physics and Astrophysics, University of Delhi, Delhi 110007, India
[b] Physics Department, Miranda House, University of Delhi, Delhi 110007, India

ARTICLE INFO

*Article history:*
Received 27 October 2015
Received in revised form
15 January 2016
Accepted 28 January 2016
Available online 29 January 2016

*Keywords:*
Nickel oxide
Low density lipoprotein
Sputtering
Electrochemical biosensor

ABSTRACT

A label-free electrochemical immunosensor, based on nickel oxide (NiO) thin film, for the detection of low density lipoprotein (LDL) has been proposed. P-type semiconducting NiO thin film was deposited by RF sputtering technique and its properties were investigated by X-ray diffraction and Fourier transform infrared spectroscopy. The NiO thin film was utilized as an efficient matrix for the covalent immobilization of apolipoprotein B-100 antibody using EDC/NHS chemistry. The immunoelectrode, thus prepared, was studied using differential pulse voltammetry, cyclic voltammetry and electrochemical impedance spectroscopy. The impedimetric response of the immunosensor exhibited a high sensitivity of 12 $k\Omega\ \mu M^{-1}$ over a wide linear range (0.018–0.5 μM) of LDL. The long shelf life (18 weeks) and enhanced performance characteristics of the immunosensor demonstrate the excellent ability of the NiO matrix for quantification of LDL at commercial level.



## 1. Introduction

Cholesterol is carried in blood plasma by different lipoproteins. Low density lipoprotein (LDL) is the most investigated as it is related with heart diseases and other ailments like atherosclerosis (Wilson, 1990; Luc et al., 2002). LDL can transport the cholesterol into artery walls which accumulates and leads to blockage of arteries, plaque ruptures and clot formation. Frequent and precise monitoring of LDL is, thus, vital for diagnostics. LDL is measured indirectly in the laboratories using the Friedewald equation by subtracting other cholesterol levels like high density lipoprotein (HDL) and triglycerides from total cholesterol (Friedewald et al., 1972). Since this is an indirect method, it does not give accurate values. There are certain direct methods being reported for LDL detection, for instance nuclear magnetic resonance (NMR) and ultracentrifugation (Daykin et al., 2001; Griffin et al., 1990; Dong et al., 2011). However, these techniques are costly and slow. Biosensors, on the other hand, offer an attractive alternative for direct detection of LDL with good sensitivity and selectivity (Cooper and Cass, 2004).

LDL is a large protein composed of cholesteryl esters, free unesterified cholesterol, triglycerides and a single protein molecule, apolipoprotein B-100. The development of immunosensors, based on interaction of LDL and its specific antibody (anti-apolipoprotein B-100), exploiting electrochemical, optical or piezoelectric transducers, has recently gained the interest of researchers (Snellings et al., 2003; Matharu et al., 2009; Jie et al., 2007). Snellings et al. (2003) fabricated a quartz crystal microbalance acoustic wave LDL sensor using dextran sulfate layer on gold surface. Jie et al. (2007) fabricated a CdS nanocrystal based electrochemiluminescence biosensor. Surface plasmon resonance technique has been employed by Matharu et al. (2009) for detection of LDL using self assembled monolayer (SAM) of 4-aminothiophenol (ATP). However, electrochemical impedimetric biosensors have an edge over others due to their label-free, simple and cost effective approach (Lisdat and Schäfer, 2008).

The performance of this biosensor in turn depends on the nature and quality of the matrix utilized for immobilization of bioreceptor. Various matrices like polyaniline, carbon nanotubes, gold and SAMs of different materials have been utilized for the development of LDL biosensors but lack stability (Matharu et al., 2010; Ali et al., 2014a, 2014b; Oliveira et al., 2011). On the contrary, metal oxides based matrices possess excellent charge transfer characteristics, high chemical stability, biocompatibility and non-toxicity (Jindal et al., 2012). However, metal oxide based matrices have not been explored for the detection of LDL besides the fact that they offer suitable microenvironment for conformal immobilization of biomolecules (Ansari et al., 2010). The morphology and electrical property of the matrix depends strongly upon the deposition technique employed for its fabrication. Physical deposition techniques such as sputtering are highly reproducible and impart precise control over morphology and functional property of

* Corresponding author.
*E-mail address:* drguptavinay@gmail.com (V. Gupta).

http://dx.doi.org/10.1016/j.bios.2016.01.071
0956-5663/

the matrix (Tyagi et al., 2012). Hence, sputtering is the most preferred growth technique for deposition of device quality oxide thin films for sensing applications. Nickel oxide (NiO) has an edge over other metal oxides because of its good biocompatibility and excellent p-type conductivity with enhanced electron communication feature (Arora et al., 2011). The present work is an attempt to realize a label-free biosensor for LDL detection using NiO thin film deposited by RF sputtering technique. Anti-apolipoprotein B antibody has been covalently immobilized over the deposited matrix using EDC-NHS method and the fabricated bioelectrode was used for efficient detection of LDL via electrochemical impedance spectroscopy technique.

## 2. Experimental

### 2.1. Materials and solutions

N-ethyl-N′-(3-dimethylaminopropyl) carbodiimide (EDC), N-hydroxy-succinimide (NHS), and bovine serum albumin (BSA) were purchased from Sigma Aldrich. Amino Propyl Triethoxy Silane (APTES) was acquired from Alfa Aesar. LDL and anti-apolipoprotein B (AAB) were procured from Merck Millipore. Phosphate buffer saline (PBS) was prepared by adjusting the proportion of monobasic sodium phosphate and dibasic sodium phosphate and adding 0.9% NaCl to the solution. Monobasic sodium phosphate, dibasic sodium phosphate and ethylene diamine tetra acetic acid (EDTA) were purchased from Sisco Research Laboratories. LDL concentrations (0.018–0.59 μM) were prepared in de-iodized (DI) water containing 50 mM NaCl and 0.01% EDTA. Anti-apolipoprotein B (AAB) (1 mg/ml) and BSA (2 mg/ml) solutions were prepared in 50 mM PBS solution of pH 7. All chemicals were used without further purification.

### 2.2. Preparation of immunoelectrode

NiO thin films were deposited on ITO coated corning glass slide (NiO/ITO) by RF sputtering technique employing a nickel target (99.999%) in pure oxygen ambient. The NiO thin films were deposited at room temperature and 20 mT pressure. The 1 cm × 1 cm area of glass slide (of size 2 cm × 1 cm) was masked for electrical contacts prior to film deposition. Thickness of the NiO thin film was optimized to obtain a uniform and continuous film as well as enhanced response and kept fixed at 90 nm (Supplementary Table 1). The antibody (AAB) was covalently immobilized on the NiO thin film (NiO/ITO) using EDC-NHS chemistry. A schematic for the preparation of the immunoelectrode is shown in Fig. 1. The NiO thin film was hydrolyzed so that OH groups can be attained on its surface. It was achieved by immersing the NiO/ITO electrode in a solution of $H_2O_2/NH_4OH/H_2O$ (1:1:5 v/v) for 30 min at 80 °C followed by rinsing with DI water and drying. Subsequently, the hydrolyzed film was silanized by immersing the electrode in 1% solution of Amino Propyl Triethoxy Silane (APTES) in toluene overnight at room temperature. The electrode was then washed with toluene to eliminate the physically adsorbed silanes from its surface and dried in nitrogen flow. 20 μl of AAB solution (1 mg/ml) prepared in PBS consisting of 0.4 M EDC and 0.1 M NHS was poured onto the electrode surface and incubated for an optimized time of approximately 3 h in a humid chamber at 27 °C for binding of AAB on the surface of NiO film. The concentration of AAB was optimized to obtain the maximum current response (Supplementary Table 2). The immunoelectrode (AAB/NiO/ITO) thus prepared, was washed thoroughly with PBS to remove any unbound or loosely bound antibody and was kept at 4 °C when not being used. The fabricated immunoelectrode was dipped in BSA solution for one hour to block any non-specific binding sites. For electrochemical response studies, the AAB/NiO/ITO immunoelectrode was incubated with 40 μl of different concentrations of LDL (0.018–0.59 μM) at 27 °C in a humid chamber for 1 h.

### 2.3. Measurements and apparatus

X-Ray diffraction (XRD) studies were performed on Bruker Discover D8 instrument for structural characterization of the film. Morphology of the thin film was investigated using Scanning electron microscopy (SEM) (Tescan MIRA3) and Atomic force mxiroscopy (AFM) (Bruker Dimension Icon). Fourier transform infrared (FTIR) spectroscopy (PerkinElmer Frontier) was used for optical characterization of the NiO thin film and to confirm the immobilization of AAB on the immunoelectrode surface. Electrochemical impedance spectroscopy (EIS) measurements were carried out on a Gamry Reference 600 Potentiostat/Galvanostat in a typical three-electrode cell configuration using the prepared immunoelectrode as working electrode, platinum foil being the counter electrode and Ag/AgCl as the reference electrode in PBS containing 5 mM $[Fe(CN)_6]^{3-/4-}$. Cyclic voltammetry (CV) and

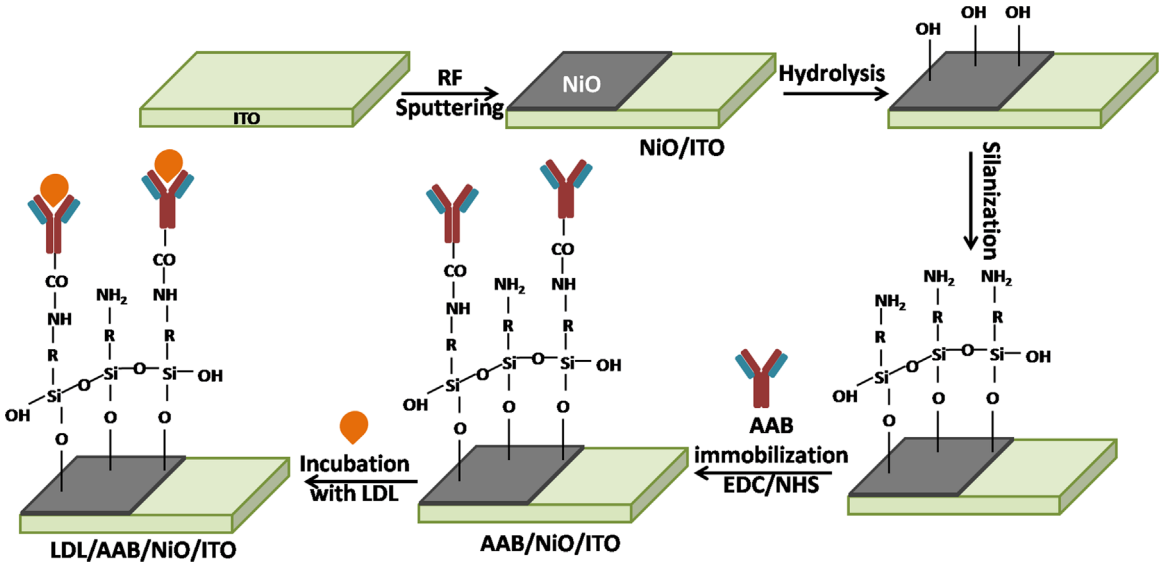


**Fig. 1.** Schematic for the preparation of the immunoelectrode and binding of LDL with the antibody AAB.

differential pulse voltammetry (DPV) studies were done in the same system but without any external mediator in PBS. Presence of redox couple in NiO ($Ni^{2+}$–$Ni^{3+}$) matrix itself facilitated the communication of electrons from the reaction site to the electrode.

## 3. Results and discussion

### 3.1. Structural and morphological characterization

The XRD pattern shown in Supplementary Fig. 1 confirms the growth of polycrystalline NiO thin film on ITO coated glass slide. The XRD peaks at $2\theta$ values of 42.7° and 62.1° correspond to the (200) and (220) planes, respectively of cubic (FCC) phase of NiO (Tyagi et al., 2012). The films are found to be preferred *a*-axis oriented. SEM and AFM images of the thin film are shown in Supplementary Fig. 2(i)–(vi). A porous morphology having uniformly distributed nanosized particles can be seen from the SEM microimage of the bare NiO thin film (Supplementary Fig. 2(i)). After immobilization of the antibody AAB, large antibody molecules in a connected mesh like form can be seen indicating the successful loading of AAB on the surface of NiO thin film (Supplementary Fig. 2 (ii)). After incubation with LDL (i.e. after measurement), a significant change in surface morphology is observed due to the binding of LDL molecules with active sites of AAB (Supplementary Fig. 2(iii)). AFM studies also confirm the formation of rough and nanoporous morphology of the bare NiO thin film (Supplementary Fig. 2(iv)). Upon antibody immobilization, the surface roughness was found to increase significantly due to the presence of macromolecules of AAB on the NiO surface of sample (Supplementary Fig. 2(v)). Further increase in surface roughness of sample was observed after incubation with LDL (Supplementary Fig. 2(vi)). The rough and nanoporous morphology of the film is advantageous for biosensing applications as it provides a larger surface to volume ratio leading to enhanced and effective loading of biomolecules (Arora et al., 2011).

### 3.2. FTIR studies

Fig. 2 displays the FTIR spectra of (i) NiO thin film and (ii) AAB/NiO thin film deposited on Si wafer under similar growth conditions. NiO thin film exhibits characteristic modes at around 445 and 668 $cm^{-1}$ (Fig. 2(i)) corresponding to stretching vibrational modes of Ni–O bond (Arora et al., 2011). The band observed at 562 $cm^{-1}$ is assigned to stretching mode of Ni–O–Ni bond (Arora et al., 2011). After immobilization of the antibody (AAB) on NiO surface, additional bands at 1665, 1528 and 1265 $cm^{-1}$ are observed which are attributed to the amide I (carbonyl stretch), amide II (N–H bending) and amide III linkages of the protein respectively (Tyagi et al., 2014) (Fig. 2(ii)). The appearance of these additional bands confirms the successful immobilization of the antibody on the surface of NiO thin film. The band appearing at around 1080 $cm^{-1}$ is related to the C=O stretching mode. The broad band present at around 3450 $cm^{-1}$ (Fig. 2(ii)) is assigned to the O–H stretching due to water molecules. This band may also be due to amide A and amide B bonds of the antibody which are reported around 3200–3300 $cm^{-1}$ (Batra et al., 2014).

### 3.3. Cyclic voltammetry studies

Cyclic voltammetry (CV) studies of NiO/ITO and AAB/NiO/ITO electrodes in the PBS solution without any external mediator are shown in Fig. 3. The corresponding curve obtained for bare ITO/glass is also shown in Fig. 3 for comparison. It is important to note that bare ITO platform does not show any redox peak which is related to the fact that ITO does not have any redox couple for the electron transfer from reaction site to the electrode. However, the CV curves for both NiO/ITO and AAB/NiO/ITO electrodes show distinct oxidation and reduction peaks (Fig. 3), which are consistent with the oxidation and reduction potential of $Ni^{2+}$ and $Ni^{3+}$ present in the NiO matrix itself (Shamsipur et al., 2010). The NiO matrix deposited in the present work by RF sputtering, thus, shows redox activity in the PBS solution without any external mediator and provides a fast electron transfer path. It is important to note that that the immobilization of AAB on the surface of NiO matrix caused a drastic reduction in the peak oxidation current (from 473 μA to 125 μA) as seen in Fig. 3. This is related to the fact that that the macromolecules of AAB restrict the flow of charge carriers. Supplementary Fig. 3 shows the CV response obtained for the AAB/NiO/ITO immunoelectrode as a function of scan rate ($\upsilon$) from 70 to 160 mV/s. The peak oxidation current ($I_{po}$) and peak reduction ($I_{pr}$) currents increase linearly with square root of scan rate (Inset: Supplementary Fig. 3) and the peak potentials are seen to shift slightly (anodic peak potential towards higher values and cathodic peak potential towards lower side). The obtained behavior indicates a diffusion controlled quasi reversible process in the present study.

The linear regression equations for the variation of peak redox currents are given below:

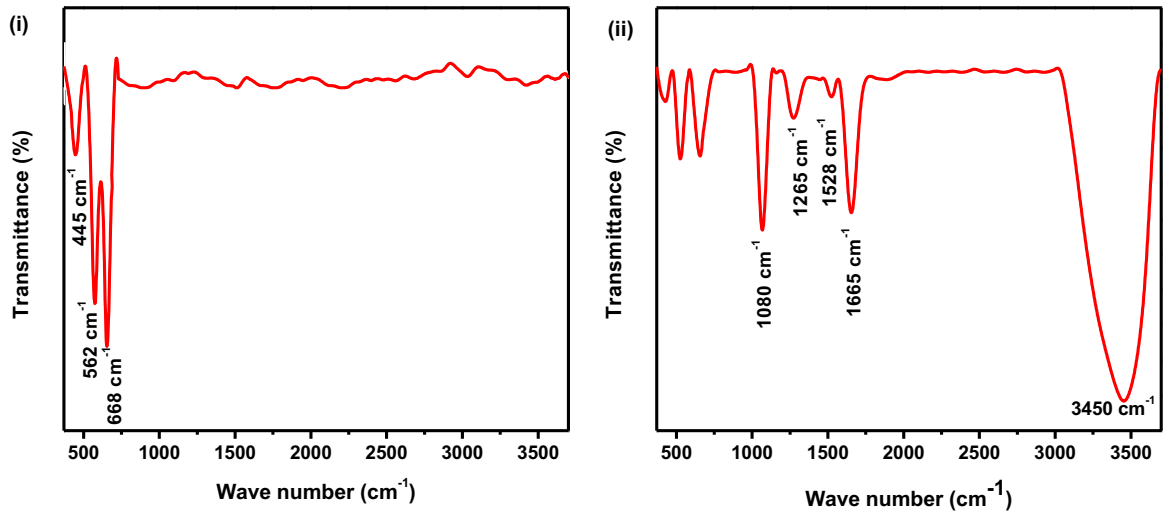


**Fig. 2.** FTIR spectra of (i) NiO thin film and (ii) AAB/NiO thin film deposited on Si wafer.

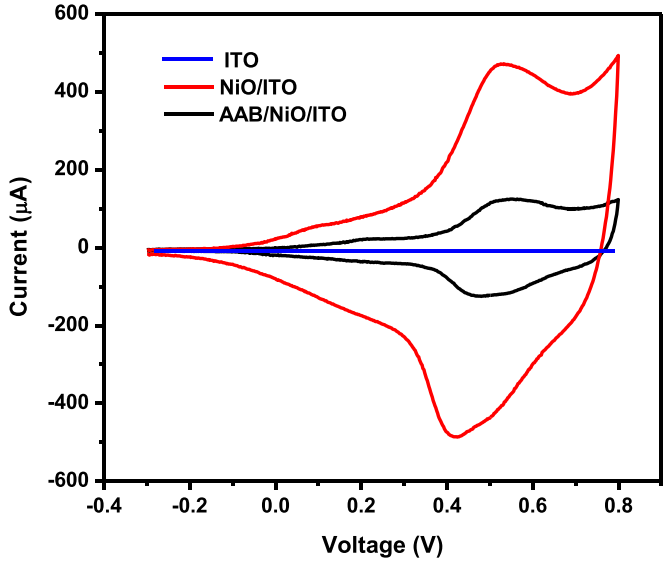


**Fig. 3.** CV curves obtained for the ITO coated glass slide, NiO/ITO electrode and AAB/NiO/ITO immunoelectrode in PBS solution without any external mediator.

$$I_{po} = 0.0261v^{1/2} + 0.135 \text{ with } R^2 = 0.995$$

$$I_{pr} = -0.0251v^{1/2} - 121 \text{ with } R^2 = 0.988$$

where $R^2$ is the regression coefficient. It may be noted that the values of $R^2$ are very close to 1 which indicates a good linear variation.

The concentration of ionic species on the surface of AAB/NiO/ITO immunoelectrode was calculated from the Brown Anson model using the equation (Bard and Faulkner, 2000)

$$I_{po} = \frac{n^2F^2\Gamma Av}{4RT}$$

where $\Gamma$ is the value of surface concentration to be estimated in mol cm$^{-2}$, $R$ is the gas constant, $T$ is the temperature, $F$ is the Faraday constant, $n$ is the number of charge carriers transferred and $A$ is the area of the electrode in cm$^2$. The values of $I_{po}/v$ was calculated from the slope of the plot between $I_{po}$ and $v$. The estimated value of $\Gamma$ was found to be about $1.41 \times 10^{-6}$ mol cm$^{-2}$, which is higher compared to corresponding values reported by other workers on LDL using other matrices (Ali et al., 2014a, 2014b). Thus, the NiO thin film matrix prepared in the present work, results in the presence of higher concentration of ionic species on the surface of immunoelectrode.

### 3.4. Biosensing response characteristics

It is seen that when LDL molecules are bound on the AAB/NiO/ITO immunoelectrode, the current reduces but this reduction is not appreciable in the case of CV measurements. Hence, Differential Pulse Voltammetry (DPV) was performed as a function of the concentration of LDL. The DPV spectra in the voltage range 0.2–0.55 V obtained for both NiO/ITO electrode and AAB/NiO/ITO immunoelectrode in PBS without any external mediator are shown in Fig. 4. A decrease in the oxidation current is noted upon immobilization of AAB antibody on NiO/ITO electrode (Fig. 4) which is in agreement with the CV studies discussed earlier (Fig. 3). Further decrease in the peak oxidation current from 311 to 55 μA is observed on incubation with different concentrations of LDL from 0.018 to 0.5 μM (Fig. 4). The continuous decrease in current for AAB/NiO/ITO immunoelectrode with increase in concentration

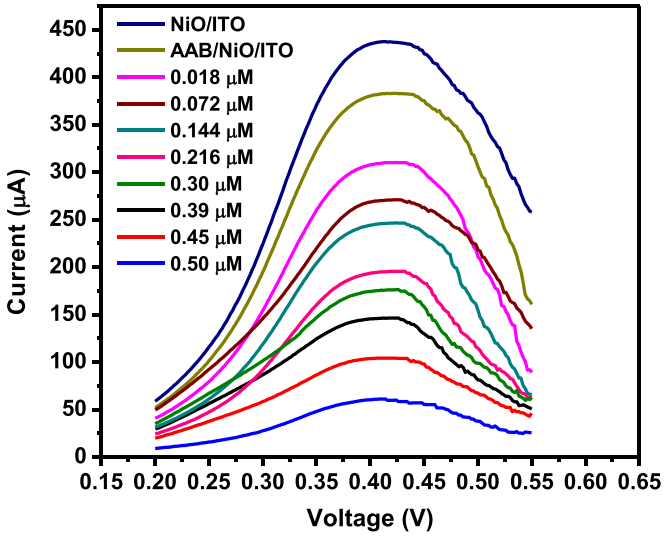


**Fig. 4.** DPV curves obtained for NiO/ITO, AAB/NiO/ITO and AAB/NiO/ITO immunoelectrode incubated with different concentrations of LDL.

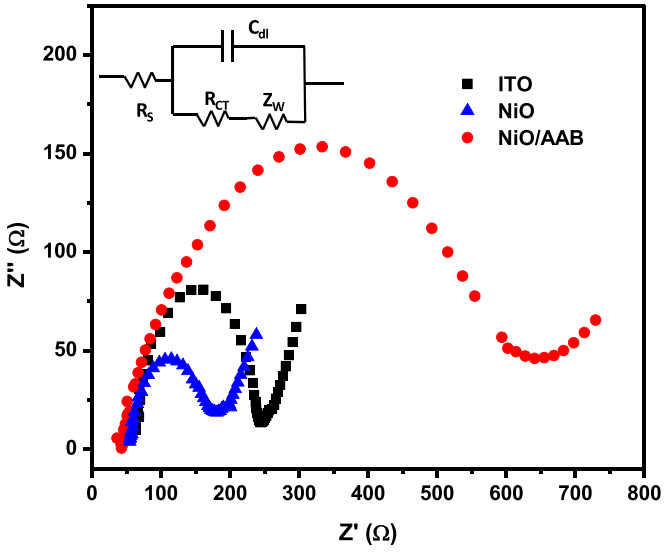


**Fig. 5.** EIS spectra of bare ITO/glass, NiO/ITO electrode and AAB/NiO/ITO immunoelectrode. Inset: shows the equivalent Randles circuit.

may be due to the formation of insulating antigen–antibody immunocomplex, which hinders the flow of charge carriers. The sensitivity of the immunoelectrode was evaluated from the DPV response and found to be about 0.46 mA μM$^{-1}$.

Fig. 5 shows the EIS curves (Nyquist plots) obtained for bare ITO/glass electrode, NiO/ITO electrode and AAB/NiO/ITO immunoelectrode in the frequency range $10^{-2}$–$10^5$ Hz. Typical semicircle behavior is observed in all the cases where diameter of the semicircle signifies the charge transfer resistance ($R_{CT}$) offered by the electrodes. The semicircle part, observed at higher frequencies, is associated with the electron transfer limited process, while the linear part seen at lower frequencies is characteristic of a diffusion limited process (Huang et al., 2006). The EIS data has been modeled using equivalent Randles circuit as shown in the inset of Fig. 5, which includes capacitance of the dielectric layer ($C_{DL}$) in series with the electrolyte resistance ($R_S$), the charge-transfer resistance ($R_{CT}$), and the Warburg impedance ($Z_W$). $R_S$ and $Z_W$ correspond to the properties of the bulk while $R_{CT}$ and $C_{DL}$ represent the properties of the electrode-electrolyte interface (Huang et al., 2006). The value of $R_{CT}$ is related to the hindrance to

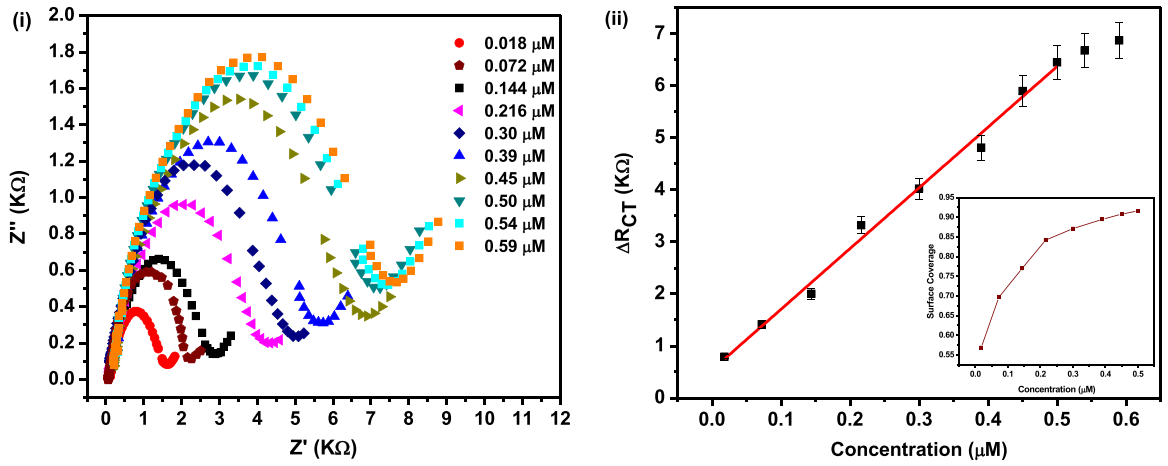


**Fig. 6.** Impedimetric response studies of AAB/NiO/ITO immunoelectrode incubated with different concentrations of LDL (ii) Calibration curve obtained between $\Delta R_{CT}$ and concentration of LDL. Inset: shows the variation of surface coverage of prepared immunoelectrode with concentration of LDL.

the current flow produced by redox reactions at the interface of prepared electrodes with PBS and was found to decrease from 182 Ω to 131 Ω when NiO matrix is deposited over ITO coated glass slide (Fig. 5). This result highlights the excellent charge transfer characteristic of the NiO matrix. After immobilization of AAB antibody on the NiO surface, value of $R_{CT}$ increases to 598 Ω confirming the successful immobilization of antibody. The presence of bulky protein molecules on the surface of NiO/ITO electrode blocks the charge transfer and leads to higher value of $R_{CT}$. These results are consistent with the CV measurements. Electrochemical impedance response studies were also conducted for AAB/NiO/ITO immunoelectrode as a function of LDL concentration and are shown in Fig. 6(i). The value of $R_{CT}$ increases linearly from 1.39 to 7.05 kΩ with increase in the concentration of LDL from 0.018 to 0.5 μM as reflected by the increase in diameter of the semicircle of the Nyquist plot. At concentrations higher than 0.5 μM, the increase in $R_{CT}$ was not linear and tended towards saturation. The observed increase in $R_{CT}$ value is attributed to the increase in accumulation of antigen–antibody immunocomplex on the surface of AAB/NiO/ITO immunoelectrode which functions as a barrier for charge communication. Moreover, LDL is negatively charged at pH 7.0 and offers electrostatic force of repulsion to the electrons transferring from negative redox couple $[Fe(CN)_6]^{3-/4-}$, thereby resulting in an increase in the $R_{CT}$ value. The observed linear range in the present work is much beyond the physiological limits (0.144–0.30 μM) of LDL (Rader and Hoobs, 2007) and hence, prepared AAB/NiO/ITO immunosensor can be employed for efficient detection of LDL. The value of $R_{CT}$ of immunoelectrode is obtained before and after incubation with LDL of different concentrations and hence, the change in $R_{CT}$ ($\Delta R_{CT}$) is evaluated. Subsequently, a calibration curve is drawn in Fig. 6(ii) between the change in $R_{CT}$ of immunoelectrode ($\Delta R_{CT}$) and the concentration of LDL. The calibration curve (Fig. 6(ii)) shows a linear variation in $\Delta R_{CT}$ from 0.79 to 6.45 kΩ over a wide range of LDL concentration (0.018–0.5 μM) and tendency towards saturation thereafter. The straight line is fitted to the data by linear regression analysis defined by the equation, $y = 12.01x + 0.55$ with a regression coefficient of $r^2$=0.991. The value of regression coefficient is found to be close to 1 indicating good linearity of the calibration curve. The sensitivity of the immunosensor was computed from the slope of the calibration curve and found to be about 12 kΩ $\mu M^{-1}$. The value of sensitivity is higher than corresponding values reported in literature for other electrodes (Matharu et al., 2010; Ali et al., 2014a, 2014b). The limit of detection of the biosensor was calculated using the expression 3 SD/S where SD is the standard deviation and S is the sensitivity and was found to be 0.015 μM. The enhanced response can be credited to the exceptional electron transfer capability of the NiO matrix prepared in the present work. The estimated values of circuit elements used in the modeling are given in Supplementary Table 3.

The surface coverage (Θ) of the LDL molecules on the surface of the AAB/NiO/ITO immunoelectrode is estimated from the following equation (Szyma´nska et al., 2007)

$$\Theta = 1 - \frac{R_o}{R_i}$$

where $R_o$ is the charge transfer resistance of AAB/NiO/ITO immunoelectrode before incubation with LDL and $R_i$ is the charge transfer resistance of the immunoelectrode after incubation with a specific concentration of LDL. Θ gives a measure of the binding sites of the antibody which are occupied by the antigen. The values of Θ were estimated for different concentrations of LDL and the corresponding curve is shown in inset of Fig. 6(ii). It can be observed that the value of Θ increases continuously from 0.56 to 0.89 with rise in the concentration of LDL from 0.018 to 0.39 μM and tends to saturate at higher LDL concentrations ( > 0.39 μM). The obtained results indicate that at higher concentrations, large number of antigens bind to the antibodies at the binding sites available on the surface of the immunoelectrode.

The association or affinity constant of antibody–antigen interaction on the surface of the immunoelectrode can be calculated using the Langmuir isotherm (Rezaei et al., 2011). It presumes all antigen binding sites to be equivalent and possessing equal energy independent of each other. In this case, Θ is related to the association constant $K_a$ by the equation (Rezaei et al., 2011)

$$\Theta = \frac{K_a c}{1 + K_a c}$$

where c symbolizes the concentration of LDL molecules. If we linearize the Langmuir isotherm and use the relation between Θ and $R_{CT}$,

$$K_a c = \frac{R_i - R_0}{R_0}$$

Association constant represents the affinity of AAB for LDL and can be estimated from the slope of the curve between relative values of $R_{CT}$ and concentration of LDL. The value of association constant is found to be about $1.8 \times 10^7\ M^{-1}$ for the NiO matrix based immunoelectrode (AAb/NiO/ITO) revealing a strong binding affinity between the two which leads to higher sensitivity.

The heterogeneous electron transfer (HET) $K_e$ can be estimated according to the equation (Bardea et al., 2000)

$$K_e = \frac{RT}{n^2F^2AR_{CT}C}$$

where $C$ is the concentration of redox probe present in the PBS solution. The value of $K_e$ was evaluated to be about $2.8 \times 10^{-4}$ cm/s for the NiO/ITO electrode, which is much higher than the corresponding values reported for CNT-chitosan based electrode (Ali et al., 2014a, 2014b). These results clearly revealed a fast electron transfer between the solution and the electrode, which in turn depends on the growth of good quality p-type NiO matrix. The value of $K_e$ was found to decrease to $8.8 \times 10^{-5}$ cm/s for the AAB/NiO/ITO immunoelectrode implying that the presence of immobilized antibody on NiO/ITO electrode offers resistance to electron transfer and provides hindrance to the $[Fe(CN)_6]^{3-/4-}$ redox couple. Similar observation was reflected from the values of electron transfer resistance ($R_{CT}$) as discussed earlier.

### 3.5. Stability, selectivity and reproducibility of the biosensor

A control experiment has been carried out to rule out the possibility of interference. The EIS and DPV measurements of the bare NiO/ITO electrode were carried out in the presence of LDL as shown in Supplementary Fig. 4(i). No significant changes in the values of $R_{CT}$ (EIS) and peak oxidation current (DPV) were observed implying that the changes observed for the AAB/NiO/ITO immunoelectrode upon incubation with LDL are due to the specific antibody–antigen binding. Also, the selectivity of the AAB/NiO/ITO immunoelectrode was studied by incubating it with HDL (50 mg/dl), VLDL (30 mg/dl) and total cholesterol (150 mg/dl) along with LDL (0.216 μM) and the corresponding data is shown in Supplementary Fig. 4(ii). Negligible changes ($< \pm 3\%$) were observed in the $R_{CT}$ values in EIS measurements (RSD of 0.96%) revealing that the fabricated sensor is highly specific and selective towards LDL. The device to device variation has been checked by preparing 5 different sensors at different times under identical conditions. Initial tests were carried out on bare NiO/ITO film using CV measurements (Supplementary Fig. 5(i)). Then, the sensors were modified by AAB and tested for a fixed concentration of LDL (0.216 μM) using EIS and the value of $R_{CT}$ was found to be almost same with a relative standard deviation (RSD) of 1.06% (Supplementary Fig. 5(ii)). The stability of the redox signal of the bare NiO thin film was investigated by taking 5 cycles in cyclic voltammetry measurements and the curve was found to exactly retrace the original curve (Supplementary Fig. 6(i)). These measurements were repeated multiple times over a period of time (1 week) and the values of peak oxidation and reduction currents were found to be same.

The prepared immunoelectrode was successfully regenerated by dipping in 0.2 M glycine buffer (Glycine-HCl) for 5 min, which dissociates the antibody–antigen immunocomplex. It was then rinsed with DI and the electrochemical measurements were taken to confirm the dissociation of the antibody–antigen complex. The regenerated immunosensor was found to be reusable for at least 15 times without any significance decrease in the value of $R_{CT}$. Hence, the p-type NiO thin film deposited by RF sputtering acts as an efficient matrix for effective immobilization of AAB antibody retaining its activity and preventing the leaching out of the antibody. The stability of the biosensor was tested by measuring the value of $R_{CT}$ for a fixed concentration of LDL (0.216 μM) at regular intervals of time (once in every 2 weeks) for a period of 18 weeks (Supplementary Fig. 6(ii)). The biosensor was stored at 4 °C when not in use. It was found to retain 90% of its activity ($R_{CT}$ value) after 18 weeks with RSD value of 1.78% demonstrating higher stability of the NiO based immunoelectrode.

## 4. Conclusion

The development of an efficient electrochemical immunosensor for the detection of LDL using NiO thin film has been successfully demonstrated. Electrochemical impedance spectroscopy, based on the formation of antibody–antigen immunocomplex, has been exploited for detection of LDL over a wide concentration range. A high sensitivity of 12 $k\Omega\ \mu M^{-1}$ and long shelf life of 18 weeks have been observed for the LDL immunosensor. The immunoelectrode is regenerative and can be efficiently used for at least 15 times without any appreciable degradation in the sensing response characteristics. The superior response characteristics of the immunosensor towards LDL can be attributed to the excellent electron transfer properties of the *a*-axis oriented NiO matrix deposited by RF sputtering technique. The prepared immunosensor holds great potential for sensitive estimation of LDL in the blood serum.

## Acknowledgments

Authors are grateful to Department of Science and Technology (DST), Government of India. One of the authors (GK) acknowledges University Grants Commission (UGC) for research fellowship.

## Appendix A. Supplementary material

Supplementary data associated with this article can be found in the online version at http://dx.doi.org/10.1016/j.bios.2016.01.071.

## References

Ali, M.A., Reza, K.K., Srivastava, S., Agrawal, V.V., John, R., Malhotra, B.D., 2014a. Langmuir 30, 4192.
Ali, M.A., Singh, N., Srivastava, S., Agrawal, V.V., John, R., Onoda, M., Malhotra, B.D., 2014b. Appl. Biochem. Biotechnol. 174, 926.
Ansari, A.A., Kaushik, A., Solanki, P.R., Malhotra, B.D., 2010. Bioelectrochemistry 77, 75.
Arora, K., Tomar, M., Gupta, V., 2011. Biosens. Bioelectron. 30, 333.
Bard, A.J., Faulkner, L.R., 2000. Electrochemical Methods: Fundamentals and Applications, 2nd Ed. Wiley, New York.
Bardea, A., Katz, E., Willner, I., 2000. Electroanalysis 12, 1097.
Batra, N., Sharma, A., Tomar, M., Gupta, V., 2014. Thin Solid Films 562, 612.
Cooper J., Cass T., 2004. Oxford University Press, USA.
Daykin, C.A., Corcoran, O., Hansen, S.H., Bjørnsdottir, I., Cornett, C., Connor, S.C., Lindon, J.C., Nicholson, J.K., 2001. Anal. Chem. 73, 1084.
Dong, J., Guo, H., Yang, R., Li, H., Wang, S., Zhang, J., Chen, W., 2011. J. Lipid Res. 52, 383.
Friedewald, W.T., Levy, R.I., Fredrickson, D.S., 1972. Clin. Chem. 18, 499.
Griffin, B.A., Caslake, M.J., Yip, B., Tait, G.W., Packard, C.J., Shepherd, J., 1990. Atherosclerosis 83, 59.
Huang, H., Liu, Z., Yang, X., 2006. Anal. Biochem. 356, 208.
Jie, G., Liu, B., Pan, H., Zhu, J.-J., Chen, H.-Y., 2007. Anal. Chem. 79, 5574.
Jindal, K., Tomar, M., Gupta, V., 2012. Biosens. Bioelectron. 38, 11.
Lisdat, F., Schäfer, D., 2008. Anal. Bioanal. Chem. 391, 1555.
Luc, G., Bard, J.-M., Arveiler, D., Ferrieres, J., Evans, A., Amouyel, P., Fruchart, J.-C., Ducimetiere, P., 2002. Atherosclerosis 163, 377.
Matharu, Z., Bandodkar, A.J., Sumana, G., Solanki, P.R., Ekanayake, E.M.I.M., Kaneto, K., Gupta, V., Malhotra, B.D., 2009. J. Phys. Chem. B 113, 14405.
Matharu, Z., Sumana, G., Gupta, V., Malhotra, B.D., 2010. Thin Solid Films 519, 1110.
Oliveira, M.D.L., Abdalla, D.S.P., Guilherme, D.F., Faulin, T.E.S., Andrade, C.A.S., 2011. Sens. Actuators, B 155, 775.
Rader, D.J., Hobbs, H.H., 2007. Kasper, D.L., Braunwald, E., Fauci, A.S. (Eds.), Harrison's Principles of Internal Medicine, Edn. 16 McGraw Hill Medical, Publishing Division, San Francisco, p. 2295.
Rezaei, B., Majidi, N., Rahmani, H., Khayamian, T., 2011. Biosens. Bioelectron. 26, 2130.
Shamsipur, M., Najafi, M., Hosseini, M.-R.M., 2010. Bioelectrochemistry 77, 120.
Snellings, S., Fuller, J., Pitner, M., Paul, D.W., 2003. Biosens. Bioelectron. 19, 353.
Szyma´nska, I., Radecka, H., Radecki, J., Kaliszan, R., 2007. Biosens. Bioelectron. 22, 1955.
Tyagi, M., Tomar, M., Gupta, V., 2012. Anal. Chim. Acta 726, 93.
Tyagi, M., Tomar, M., Gupta, V., 2014. Biosens. Bioelectron. 52, 196.
Wilson, P.W.F., 1990. Am. J. Cardiol. 66, A7.